

# Whole Skin Locomotion Inspired by Amoeboid Motility Mechanisms

Dennis W. Hong

Mark Ingram

Derek Lahr

Mechanical Engineering Department (0238),  
Virginia Tech,  
Blacksburg, VA 24061

*In this paper, a locomotion mechanism for mobile robots inspired by how single celled organisms use cytoplasmic streaming to generate pseudopods for locomotion is presented. Called the whole skin locomotion, it works by way of an elongated toroid, which turns itself inside out in a single continuous motion, effectively generating the overall motion of the cytoplasmic streaming ectoplasmic tube in amoebae. With an elastic membrane or a mesh of links acting as its outer skin, the robot can easily squeeze between obstacles or under a collapsed ceiling and move forward using all of its contact surfaces for traction, even squeezing itself through holes of a diameter smaller than its nominal width. Therefore this motion is well suited for search and rescue robots that need to traverse over or under rubble, or for applications where a robot needs to enter into and maneuver around tight spaces such as for robotic endoscopes. This paper summarizes the many existing theories of amoeboid motility mechanisms and examines how these can be applied on a macroscale as a mobile robot locomotion concept, illustrating how biological principles can be used for developing novel robotic mechanisms. Five specific mechanisms are introduced, which could be implemented to such a robotic system. Descriptions of an early prototype and the preliminary experimental and finite element analysis results demonstrating the feasibility of the whole skin locomotion strategy are also presented, followed by a discussion of future work. [DOI: 10.1115/1.2976368]*

## 1 Introduction

As the technology of robotics intelligence advances and new application areas for mobile robots increase, the need for alternative fundamental locomotion mechanisms for robots that can enable them to maneuver into complex unstructured terrain becomes critical. Current methods of ground vehicle locomotion are based on wheels, tracks, or legs, and each of these methods has its own strengths and weaknesses [1]. In order to move a robot into an area of complex terrain, such as a collapsed building or a person's digestive tract, a new method of locomotion is needed. To be able to find people trapped in a collapsed building, a robot would need to be able to move over, under, and between rubble. Current methods of locomotion can do some of these, but they have only had limited success in all of them.

This paper presents a locomotion mechanism for mobile robots inspired by how certain single celled organisms such as amoeba generate motion for locomotion. In general, single celled organisms utilize one of three primary methods for locomotion using flagella, cilia, or pseudopods. A flagellum is a single tail that drives itself like that of a tadpole. Cilia are small hairlike strands that are used for swimming or crawling. The locomotion method of most interest to this research is the use of a pseudopod, a "fake foot" formed when part of a cell extends itself in relation to the rest of the cell body [2,3]. Pseudopods are formed by a process called cytoplasmic streaming, a process in which endoplasm (the liquid on the inside of the cell) flows forward through the cell to force the pseudopod tip outward, away from the body [4,5].

The whole skin locomotion (WSL) is an alternative fundamental locomotion mechanism for mobile robots inspired by the motility mechanisms of single celled organisms that use cytoplasmic streaming to generate pseudopods for locomotion. The name,

whole skin locomotion, comes from the fact that the entire outer surface of the robot, which has a body in the shape of an elongated torus, is used as a surface for traction and is actuated through cyclical contractions and expansions of the actuators themselves. This is fundamentally different from the undulatory motion of snakes [6,7] or inchworms [8] as WSL works more like a three-dimensional tank tread.

Since the entire skin is used for locomotion, the robot can move as long as any surface of the robot is in contact with the environment, be it the ground, walls and obstacles on the side, or the ceiling. With an elastic membrane or a mesh of links acting as its outer skin, the robot can easily squeeze between obstacles or under a collapsed ceiling and move forward using all its contact surfaces for traction. It is even possible for the robot to squeeze itself through holes with diameters smaller than its nominal width [9]. This makes WSL well suited for search and rescue robots to traverse over or under rubble, or for applications where a robot needs to maneuver itself into tight spaces, such as for robotic endoscopes [10,11] or pipe inspection robots [12]. In robotic endoscope applications, since the gastrointestinal tract is very delicate and has a complex geometry, WSL could be used to minimize the possibility of damage as it distributes the force required for movement over the largest possible area and morphs its shape to match that of the gastrointestinal tract.

Some examples of robots that use the idea of distributed contact locomotion include the rolling stent endoscope [13], a cylindrical robot with feet distributed over the surface [14,15], and a steerable monotread robot [16]. The rolling stent endoscope uses a "rolling donut" constructed from three stents positioned around the endoscope tip for intestinal locomotion, while the cylindrical robot with distributed feet performs a coordinated shoveling motion that provides forward propulsion wherever a foot is in contact with the environment. All of these robots share some similar characteristics with WSL in a sense; however, their topology and method of actuation are completely different.

This paper presents the research work toward the development of the WSL robot. First, the many existing theories of amoeboid motility mechanisms are summarized, and ideas for applying

Contributed by the Mechanisms and Robotics Committee of ASME for publication in the JOURNAL OF MECHANISMS AND ROBOTICS. Manuscript received April 6, 2008; final manuscript July 1, 2008; published online September 5, 2008. Review conducted by Jian S. Dai. Paper presented at the ASME 2005 Design Engineering Technical Conferences and Computers and Information in Engineering Conference (DETC2005), Long Beach, CA, September 24–28, 2005.

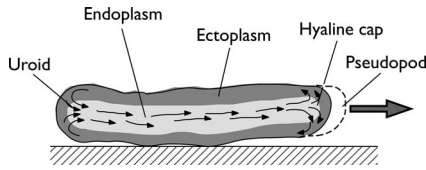


Fig. 1 Motility mechanism of a monopodial amoeba

these on a macroscale as a mobile robot locomotion concept is examined, illustrating how biological principles can be used for developing novel robotic mechanisms. Five specific mechanisms are introduced, which could be implemented to such a robotic system. Descriptions of an early prototype and the preliminary experimental and finite element analysis (FEA) results using an incremental loading approach are also presented, demonstrating the feasibility of the whole skin locomotion strategy.

## 2 Theories of Amoeboid Motility Mechanisms

The inspiration for the locomotion strategy described in this paper comes from the motion of certain single celled organisms such as the large fresh water amoeba pseudopods, *Amoeba proteus* (giant amoeba) or *Chaos chaos*. Most of the research on amoeba locomotion has been done on these particular species because of their large size (up to and larger than 1 mm). Speculation about how amoebae generate motion for locomotion began in 1842 [17], and many theories of amoeboid motility mechanisms have been proposed [4,5,18]. Among them, two of the most useful models for adapting and implementing motion on a macroscale are presented here. These are the tail contraction model and the frontal-zone contraction model.

**2.1 Cytoplasmic Streaming.** In both the tail contraction model and the frontal-zone contraction model, the motion of the body is caused by the process of cytoplasmic streaming. Cytoplasm is made up of both a gel-like ectoplasm and a liquid form endoplasm. The endoplasm flows forward inside the ectoplasmic tube, which acts as the outer skin. When the endoplasm reaches the front, it turns into a gel-like ectoplasm, forming the pseudopodial tip in a region called the hyaline cap, which in turn causes the ectoplasmic tube to move forward. As the amoeba advances, the ectoplasmic tube turns into a liquid form endoplasm at the rear, or uroid of the cell, and the process continues [4,5]. The net effect of this ectoplasm-endoplasm transformation is the forward motion of the amoeba, as shown in Fig. 1.

Most researchers in the field agree that the motor for the motion of amoeba is actomyosin based. Actomyosin is a protein complex in muscle fibers composed of myosin and actin and shortens when stimulated and causes muscle contractions in biological systems [4,5,19]. Exactly how the actomyosin based cytoplasmic streaming happens is still being debated and many theories exist. However, the tail contraction model and the frontal-zone contraction model are the two theories presented here.

**2.2 Tail Contraction.** The tail contraction model (also called ectoplasmic tube contraction), first put forward by Ecker [17,20],

is based on the observable contraction of the rear of the cell. While the amoeba is moving, the membrane around the uroid folds up as the ectoplasm immediately under it turns into an endoplasm. This folding characterizes the uroid and can be observed in any moving amoeba. It is believed that as the tail contracts, it causes a small positive pressure within the cytoplasm, which forces more fluid endoplasm forward along the line of least resistance.

This theory was supported by basic observations of a moving amoeba and in experiments where particles implanted in the cytoplasm come closer together in the uroid, indicating contraction of the cytoplasm [21]. The pressure gradient caused by the contraction can be measured by having an amoeba crawl through a hole between two chambers and by measuring the pressure difference [5].

**2.3 Frontal-Zone Contraction.** The frontal-zone contraction model attempts to explain the underlying mechanism of the assembly process of the endoplasm into the gel-like ectoplasm at the advancing tip (hyaline cap) of the pseudopod, which, accompanied by contraction, pulls the endoplasm forward and pushes the pseudopod tip outward. This theory was proposed after an experiment in 1960, which could not be explained by the tail contraction model [18]. In this experiment, the membrane of an amoeba is broken, and it was shown that the cytoplasm was still able to flow in multiple directions even without the contracting uroid. This suggests that the tail contraction model is not the only mechanism for cytoplasmic streaming [19,22]. Other experiments followed, further showing that the pressure gradient was not the sole driving force behind amoeboid locomotion [17,23,24]. However, there are still no direct evidence showing either theory to be entirely complete, and thus the debate on the amoeboid motility mechanism continues.

## 3 Whole Skin Locomotion

Inspired by the cytoplasmic streaming motility mechanism of monopodial single cell organisms like the amoeba, the WSL is developed as an alternative locomotion strategy for mobile robots. Directly imitating the tail contraction model or the frontal-zone contraction model of the cytoplasmic streaming process is very difficult, if not impossible, on a macroscale. Thus, instead of using the process of the liquid to gel transformation of cytoplasm, a similar motion is implemented with a flexible membrane skin (or a mesh of links) in the shape of an elongated torus. The skin of this torus moves with an everting motion, turning itself inside out in a single continuous motion, effectively generating the overall motion of the cytoplasmic streaming in the amoebae, as seen in Fig. 2. This toroid shaped skin has either an enclosed concentric solid tube (CST) or is fluid filled (fluid filled toroid model). The motion of the fluid filled toroid model is similar to that of a common child's toy that is often referred to as a "water worm."

The motion of the torus shaped skin is generated by contracting and expanding the skin itself or by actuation rings embedded in the skin. As the WSL mechanism converts this contracting and expanding motion of a ring shaped actuator to a toroidal everting motion, it is difficult to implement this using conventional actua-

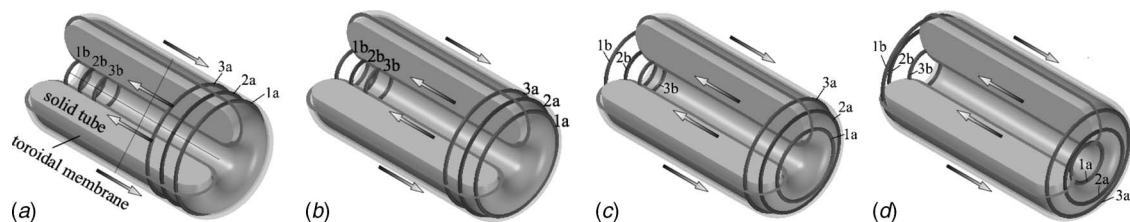
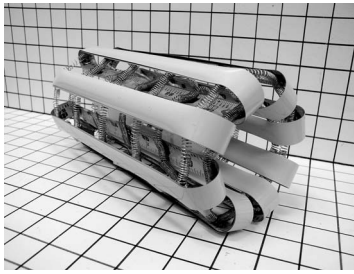


Fig. 2 Motion generated by the rear contractile rings (1a, 2a, and 3a) and frontal expansile rings (1b, 2b, and 3b) for the concentric solid tube model



**Fig. 3** An early WSL prototype using a statically balanced closed-loop tape spring mechanism with shape memory alloy actuators

tors such as electric motors and linear actuators. Instead, special rings of accordion-type hose that are expanded and contracted using pressurized fluid [3] are used for larger scale implementations, and rings of electroactive polymer (EAP) strips around the toroid [25] are used for smaller scale applications. Figure 3 shows an early prototype using shape memory alloy actuators. These actuators are used for generating the everting motion of the skin using several different mechanisms as presented next.

### 3.1 Rear Contractile Rings With Concentric Solid Tube.

One mechanism of generating the motion of the toroid shaped skin with the CST model is to use contractile rings embedded into the skin. As the rings located in the rear contract in sequence, as shown in Fig. 2, the tension in the rings generates a force in the outer skin, drawing it to the rear of the robot and creating a forward motion [26].

As the contractile ring (1a) near the edge begins to contract, it pulls itself over the rounded edge of the concentric solid tube, pulling the currently inactive rings behind them, as shown in Fig. 2(a). When the following contractile ring (2a) approaches the rounded edge, it begins to contract, adding to the force of the first ring, as shown in Fig. 2(b). This process continues as the first rings begin to pass completely inside the tube, as shown in Fig. 2(d). The active rings will continue to pull the inactive rings allowing, for continuous motion. This mechanism is very similar to the tail contraction model of the cytoplasmic streaming amoeba. However, the tension in the ring is converted to the actuating force through the direct interaction with the surface of the solid tube inside the skin.

### 3.2 Frontal Expansile Rings With Concentric Solid Tube.

This mechanism works in the opposite way to the rear contractile ring method with the CST. As the actuating rings embedded in the skin near the front (rings 1b, 2b, and 3b in Fig. 2) expand in sequence against the CST, they generate a tension in the skin on the inner side of the torus, generating the forward motion of the body. Since flexible members generally transfer force through tension only and not through compression, the expansile ring method may be less effective than the contractile ring approach due to buckling effects [26]. Nevertheless, the expansion of the rings located in the front is necessary so as to not over constrain the motion of the skin. It should be noted that the frontal expansile ring mechanism is not exactly analogous to the frontal-zone contraction theory for the monopodial cytoplasmic streaming amoeba.

**3.3 Wave Contractile/Expansile Rings With Concentric Solid Tube.** In both the frontal expansile and rear contractile actuation methods with the CST model, only a small number of the actuators generate work at any given time, those at either the front or the rear of the robot. By using a CST formed with a sinusoidal wave shape on the inner and outer surfaces, one can increase the number of active actuators and thus the overall effectiveness of the mechanism. This would allow nearly all of the actuating rings

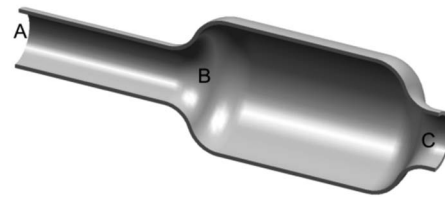


**Fig. 4** Construction of the pretensioned elastic skin fluid filled toroid model

to drive the skin simultaneously, taking advantage of the whole surface of the robot and improving the overall effectiveness of the mechanism.

**3.4 Rear Skin Contraction With Internal Fluid.** While the mechanics of the CST based actuation methods are fairly straightforward, replacing the CST with a fluid can provide certain benefits. First, it will eliminate the friction caused at the interface between the skin and the solid tube, and second, it will allow the necessary compliance for the robot to squeeze between obstacles and better conform to its environment. With a fluid filled toroid skin, the mechanisms that generate motion in the skin change significantly from the models used with the concentric solid tube model. The actuating rings on the outside would compress the rear end, which will cause the flow of the liquid forward, pushing out the inner skin in the front forward, generating the motion of the skin [27]. This is analogous to squeezing toothpaste out of a tube, while the tube continuously reforms at the front. This approach is the closest to the tail contraction theory for the cytoplasmic streaming amoeba.

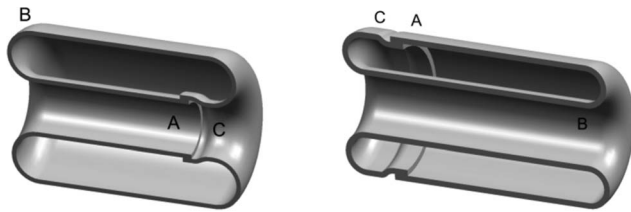
**3.5 Closed-Loop Tape Spring Mechanisms.** Another model that is being investigated is a novel single degree-of-freedom everting mechanism that utilizes a statically balanced tape spring mechanism [28]. An early prototype is shown in Fig. 3. This prototype is constructed with a number of twofold closed-loop tape spring mechanisms [28] arranged in a circular pattern, held together by actuation rings made of shape memory alloy springs in tension. Tape spring mechanisms, used in a number of recently proposed deployable structures [29] such as satellite antennas, are fully compliant mechanisms composed with a thin-walled strip having a zero longitudinal curvature and a constant transverse curvature, such as those found in tape measures. By joining the ends of a tape spring together, a closed-loop tape spring is formed. The localized folds serve as compliant revolute joints that can freely move along the length of the links, and the unfolded straight segments serve as links with variable length. The unique properties of the closed-loop tape spring mechanism enable the structure to be hollow inside and at the same time hold its shape while rotating clockwise or counterclockwise to allow the everting motion required for the WSL.

## 4 Preliminary Experiments With Internal Fluid Model

**4.1 Feasibility Experiment With Pretensioned Elastic Skin.** A simple experiment was conducted using a long elastic silicone toroid filled with water to demonstrate the feasibility of the locomotion mechanism [9]. The elastic silicone skin is formed such that the nominal diameter along half the length is smaller than the remaining half. That is, Sec. AB has a diameter half that of Sec. BC, as shown in Fig. 4.

The two ends of the tube (A and C) are then pulled together, causing the skin to roll into itself and form a long toroid shaped membrane, as seen in Fig. 5. The ends are sealed together, and the interior is filled with water.

As the toroid undergoes the everting motion, it passes through a high or a low potential energy state, corresponding to when the initially smaller inner membrane is on the outside or inside of the



(a) State of low potential energy (b) State of high potential energy

**Fig. 5 Energy states for two different positions**

mechanism, respectively, as seen in Fig. 5. When the tubular section of the smaller diameter (Sec. AB) is rolled into the center and the section of the larger diameter (Sec. BC) is rolled outward to form the outer skin, the model assumes the lowest energy state, as shown in Fig. 5(a). However, when the entire skin is rotated and flipped "inside out" such that the section of the larger diameter (Sec. BC) is rolled into the center and the tubular section of the smaller diameter (Sec. AB) is rolled outward, the outer elastic skin is now stretched, assuming the high potential energy state, as

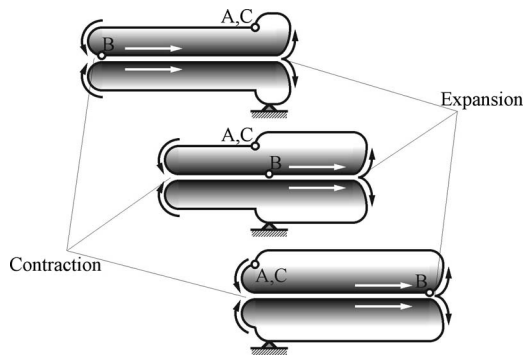


**Fig. 6 Motion of the pretensioned elastic skin fluid filled toroid model**

shown in Fig. 5(b).

Starting from this position, with a slight bias to direct the motion to the right (first figure in Fig. 6), the skin of the fluid filled toroid rotates to reach its lowest energy state (last figure in Fig. 6), moving the toroid to the right like a three-dimensional tread.

The mass of the fluid filled toroid model used for the experiment is 0.369 kg with a length of 25 cm and a nominal outer diameter of 5 cm. A sequence of pictures of the actual motion of this pretensioned skin model is shown in Fig. 7. The model traveled the distance of its full length of 25 cm in 0.46 s. This simple demonstration shows the feasibility of the locomotion mechanism for the fluid filled toroid model. With a continuous contractile actuation of the outer skin in the rear, the toroid will be able to continuously move in the forward direction.

#### 4.2 Rear Skin Contraction Experiment Using Tension

**Cords.** Another simple experiment was conducted to demonstrate the feasibility of generating the forward motion by the active contractile actuation of the outer skin. The apparatus used in this experiment was a jig, as seen in Fig. 8, with a number of tension cords wrapped around the fluid filled toroid such that when the cords are pulled, the loops will contract the outer skin to generate the necessary tension to change the potential energy state as in the previous experiment described above. Small pieces of vinyl tubing were placed between the model and the cords to prevent crimping of the outer skin between the tightening cords and to evenly distribute the contracting force over the skin. By pulling the cords in sequence to contract the outer skin, the fluid filled toroid moved forward.

From these experiments, it was found that as the cords are tensioned from the rear moving forward, the outer skin is contracted in such a way that the fluid inside the body is squeezed forward as toothpaste is dispensed from its tube. This forward motion of the internal fluid then pushes the inner skin forward, creating a forward motion of the body. This is another mechanism of motion for the rear skin contraction with the internal fluid model, which is analogical to the ectoplasmic tube contraction model of amoeba.

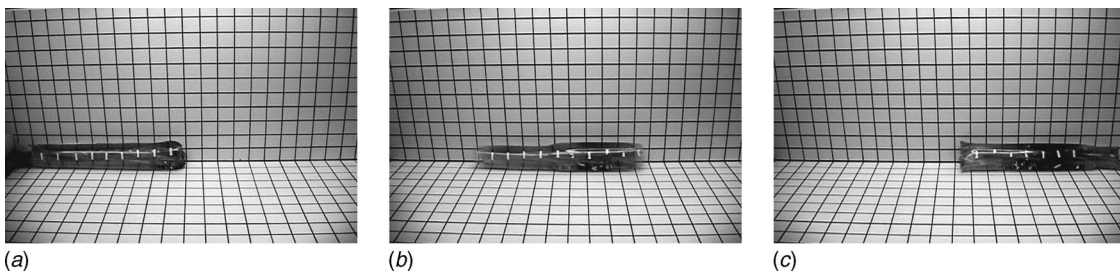


**Fig. 7 Sequence of pictures of the locomotion of the pretensioned elastic skin model. (a) At 0.0 s, (b) at 0.30 s, and (c) at 0.46 s.**

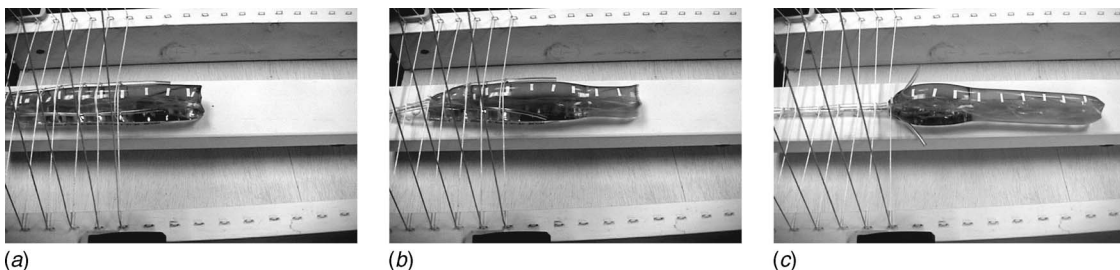


**Fig. 8 Sequence of pictures of the tension cord actuated model locomotion**

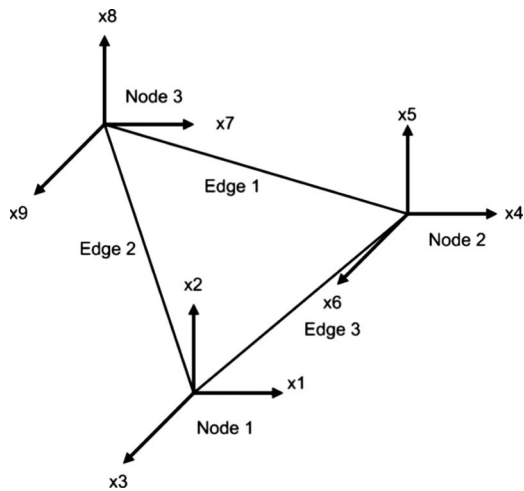


Fig. 9 Triangular element used for a 3D analysis

## 5 Finite Element Analysis Using the Incremental Loading Approach

As was stated earlier, when the robot is fluid filled, its shape and motion are determined by the internal fluid pressure, the tension in the skin, and the force generated by the actuators embedded in the skin. From the previous experiments and biological studies, specifically of the tail contraction method, one would expect that a generally contractile force generated by these EAP strips at the rear of the robot would cause this end to taper down and generate a forward motion.

Although the experiments showed us the validity of the concept, it is difficult to quantify the generated motion or the shape generated by the actuator forces. Stated differently, the interactions between the skin, fluid, ground, and actuators are not well understood. This is the driving force behind the research to develop a finite element model, which can incorporate the statics and dynamics of the hyperelastic skin, fluid filled interior, and smart material actuators. It is also hoped that the development of the FEA model will give us some insight into the underlying mechanisms within the skin and fluid that generate this motion.

**5.1 Membrane Based Finite Elements.** The membrane described here is a flat, thin structure, which exhibits only in-plane stresses and no bending stiffness [30,31]. The element model presented within this paper was originally presented by Arcaro [32]. In this formulation, the mesh consists of triangular elements, each with three nodes having three degrees of freedom apiece, as seen in Fig. 9. From the displacements, the strain is derived using Green's strain, which results in a nonlinear formulation of elements. At this point in time, a linear Hookean elastic material model is used to develop the strain energy equation; however, a nonlinear material model will be implemented in the future to better represent the actual mechanics of the WSL robot membrane.

**5.2 Loading and Boundary Conditions.** The loading of a highly elastic structure must be done carefully, especially when the direction of the loads is closely related to the shape of the structure, as with the normal force generated from an internal pressure. Being that this model contains both an internal pressure and a highly elastic membrane structure, great care was taken to ensure that the loads were appropriately applied. The method used herein is generally called "incremental loading." As the name implies, the load is gradually and incrementally increased from zero to its final value. At each iteration, the direction and magnitude of the load are updated for the most recent configuration and nodal location. In this way, as the membrane is "inflated" from its static unstressed position, the direction of the pressure loads acting on

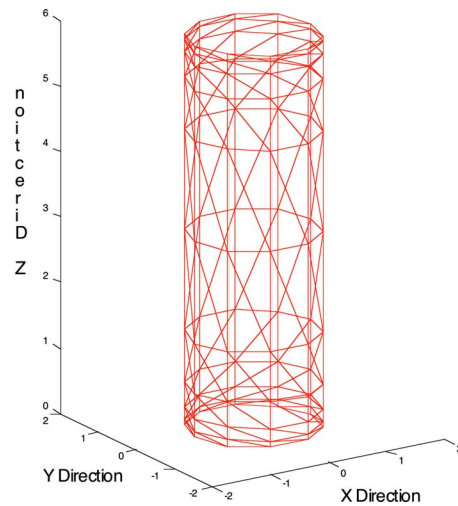


Fig. 10 Initial configuration of the unstressed WSL membrane

the surface can be updated.

The two dominant loading mechanisms in this model were the pressure loading and the circumferential stress contributed by the EAP actuators. The loads from the actuators were applied radially to nodes placed at the location of the actuators themselves. It is therefore fairly straightforward to compute the nodal forces from these loads.

At this point the only interaction with the ground considered was that with the portion of the membrane on the internal side of the robot. That is to say, the interior of the WSL robot can be thought of as being fixed to a pipe. This simplification was made so that the intricacies of the model would not be overwhelming. It is believed though that the fundamental physics underlying the everting motion can still be ascertained from this simplified model. In reality, the reaction force will most likely be generated by the friction from the weight of the robot on a flat surface. The fundamental physics of the everting motion though should remain the same regardless of the application site of the reaction force.

Figure 10 shows the unloaded cylindrical membrane structure. Boundary conditions are applied to the top and bottom-most nodes, those on the ends of the cylindrical membrane. In this case, these nodes are fixed in all three directions and are therefore not free to move. This is nearly equivalent to affixing the inner surfaces of the elongated torus to the aforementioned pipe on which the WSL robot is moving.

**5.3 Incremental Iteration Termination.** It is, of course, necessary to determine a point of termination of the incremental loading strategy. The program ends when the volume within the membrane reached a certain value. This is derived from the fact that the WSL robot is filled with a fluid that is assumed to be incompressible. Therefore any configuration that the membrane takes must have the same total volume.

**5.4 Preliminary FEA Results.** The WSL mechanism considered here begins as an unstretched cylindrical membrane 6 cm long and 2 cm in diameter. The program was first run for six incremental steps, each one with an increasing pressure. No actuator loads were considered initially to reduce the chance of error. The mesh size was refined over several runs until convergence was achieved. For these preliminary models, a mesh with 11 rings, each with ten nodes, proved satisfactory. The mesh size was reduced at the ends of the model in order to achieve a better resolution and to more accurately model the curvature at the ends of the robot. Figures 10–13 show the progression of the inflation from an unstressed state to a fully inflated form. In its final state, the membrane has stretched to nearly 4 cm in diameter and has

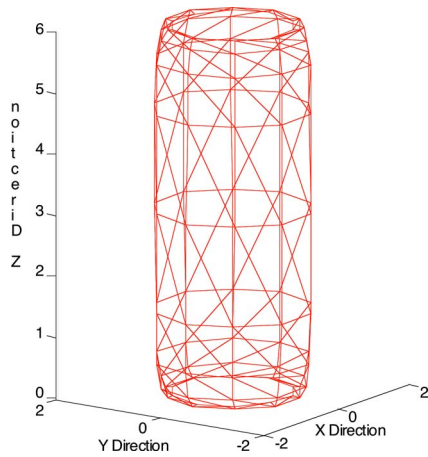


Fig. 11 Partially inflated membrane

grown to 6.2 cm long due to the ballooning toroid end caps.

The ballooning action of the membrane is as one would have expected. One can see in Figs. 10 and 11 that the cylinder begins to stretch in the radial direction, but at this point the ends have not rolled over and the defining toroidal shape of the WSL robot has not been reached. With increased internal pressure, as seen in Fig. 12, the membrane becomes fully inflated, while the ends form the “caps” of the elongated torus shape. It is believed that the caps of the elongated torus are fundamental to the everting motion of this robot because they form the transition from the inner membrane (the fixed interior of this model) to the outer membrane. Therefore, any forces generated, which allow the inner membrane to move in relation to the outer membrane or vice versa, should pass through this membrane. It is therefore important that they appear in the model as the membrane is inflated.

After the initial inflated but unactuated membrane shape had been verified, the actuator loads were applied. These loads were applied to nodes on only one end of the robot in an inward radial direction. This loading mimics the contractile force generated by EAP actuators. Loading only one end of the membrane ensures an asymmetric shape that can generate a forward motion. To maintain the volume constraint, the internal pressure was also

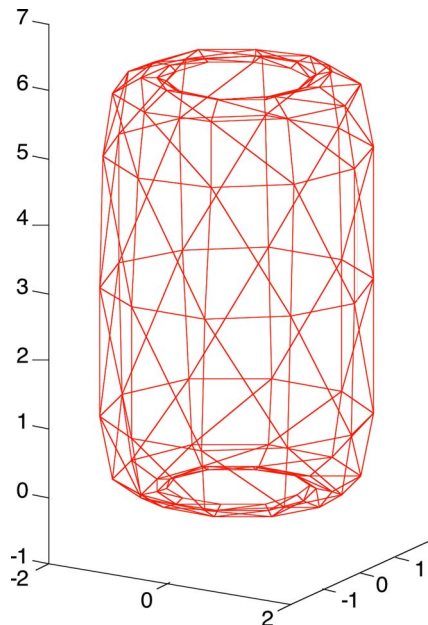


Fig. 12 Fully inflated membrane

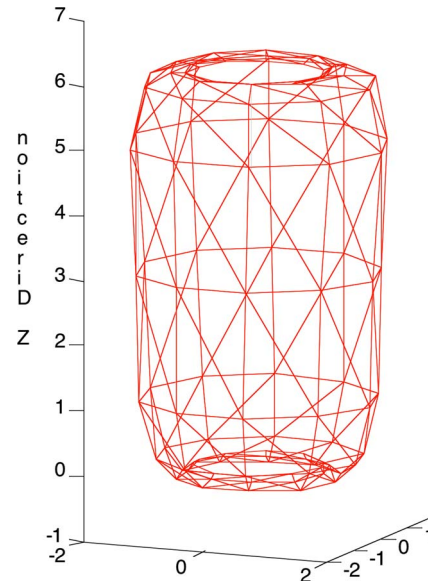


Fig. 13 Membrane under applied pressure and actuator loads exhibiting the characteristic tapered shape as compared to Fig. 14

increased from the previously described loading strategy. This is to be expected and mirrors a similar phenomenon seen in experiments in which the outer membrane becomes noticeably more taut as one end is squeezed, indicating an increase in internal pressure. Figure 13 shows the actuated results as compared to the unactuated shape in Fig. 12. Figure 14 is a cross sectional view used to better illustrate the motion the membrane undergoes as the actuators are applied.

Studying Figs. 13 and 14, one can see a slightly tapered shape of the lower section of the robot that results from the actuator loads on that end. The numerical results are more interesting. To predict the motion of the robot, one must look at the maximum and minimum positions of the membrane with respect to the fixed nodes, which are located at 0 cm and 6 cm on the  $z$ -axis at the ends of the membrane. When unactuated, the membrane was symmetric about the midplane of the robot, with the curved torus caps extending 0.086 cm beyond these ends. When loaded though, the lower end extended as far as 0.2 cm below the lower fixed nodes, and the upper end receded such that it was only 0.07 cm above the upper fixed nodes. In other words, the outer membrane moved down in the negative  $z$ -direction as much as 0.1 cm with respect to the inner membrane. Therefore, if the outer membrane were fixed by the static friction between itself and the ground, for instance, the inner membrane would be seen advancing forward, resulting in a net forward motion of the robot. Additionally in Fig. 14, it can be seen that the lowermost nodes move inward by up to 0.15 cm, while the uppermost nodes expand outward by up to 0.06 cm. Although this FEA based motion is small in comparison to a complete eversion, some conclusions can still be drawn from this pre-

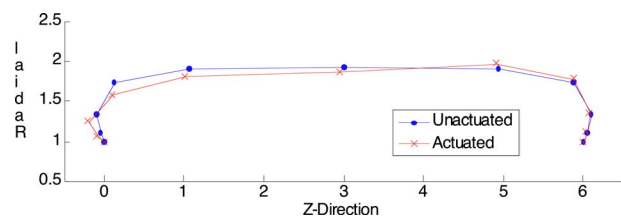


Fig. 14 Cross sectional view of the membrane surface showing the relationship between the unactuated and actuated states

liminary work due to the cyclical nature of the everting motion.

It is possible to extrapolate a complete eversion from the portion of motion studied here. If the actuation strategy were to continue along the membrane in an appropriate fashion, one would see the nodes on the lower torus cap continue to move inward, down, and into the center of the robot as the actuators continued to contract. Simultaneously, the upper torus caps would begin to draw the inner portion of the membrane upward in the  $z$ -direction and outward radially due to the increased internal pressure. These results confirm the accuracy of the membrane model with respect to physical experiments discussed earlier in that they both show similar fundamental relationships between their shape and motion. It also validates the incremental loading and termination strategy employed, which is fundamental to understanding this motion using FEA tools.

## 6 Conclusion and Future Work

A locomotion mechanism for mobile robots inspired by how single celled organisms such as amoeba use cytoplasmic streaming to generate pseudopods for locomotion is presented. Named whole skin locomotion, it works by way of an elongated toroid, which turns itself inside out in a single continuous motion, effectively generating the overall motion of the cytoplasmic streaming ectoplasmic tube in amoebae. This strategy allows the entire surface of the robot to generate traction, allowing it to traverse a complex terrain that wheeled, tracked, or legged vehicles are unable to access.

This paper summarizes the many existing theories of amoeboid motility mechanisms and examines how these can be applied on a macroscale as a mobile robot locomotion concept, illustrating how biological principles can be used for developing novel robotic mechanisms. Five actuation strategies are presented with preliminary experiments and their results, demonstrating the feasibility of the whole skin locomotion strategy. This paper also details the development of a nonlinear finite element model, which will allow the study of the interaction of the membrane and actuators and predict the shape and motion of the robot under various actuation strategies. A simple membrane element was developed and an incremental loading strategy employed to model the displacement dependent pressure and actuator loads. It was shown that a strictly contractile force at the aft end of the robot will generate a forward motion.

Research on this project continues with a focus on the finite element, analytical, and experimental models of the fluid filled WSL mechanism. The finite element code discussed in this paper is being refined and further developed with more capable and representative element and material models. In addition, an analytical solution is being sought to determine the overall shape of the unactuated membrane, including the buckling effects apparent at the ends of the robot. Finally, the design of an actuated prototype constructed from silicone rubber and shape memory alloys has begun to validate the aforementioned models and research on the robot's suitability in various applications.

## Acknowledgment

The authors would like to thank the National Science Foundation for their support for this work under Grant No. CMMI-0643839.

## References

- [1] Laney, D., and Hong, D. W., 2005, "Kinematic Analysis of a Novel Rimless Wheel With Independently Actuated Spokes," Proceedings of the 29th ASME Mechanisms and Robotics Conference, Long Beach, CA, Sept. 24–28.
- [2] Hong, D. W., 2006, "Biologically Inspired Locomotion Strategies: Novel Ground Mobile Robots at RoMeLa," Proceedings of the Third International Conference on Ubiquitous Robots and Ambient Intelligence, Seoul, South Korea, Oct. 15–17.
- [3] Ingram, M., and Hong, D. W., 2005, "Whole Skin Locomotion Inspired by Amoeboid Motility Mechanisms," Proceedings of the 29th ASME Mechanisms and Robotics Conference, Long Beach, CA, Sept. 24–28.

- [4] Allen, R. D., 1973, "Biophysical Aspects of Pseudopodium," *The Biology of Amoeba*, K. W. Jeon, ed., Academic, New York, pp. 201–247.
- [5] Lackie, J. M., 1986, *Cell Movement and Cell Behavior*, Allen and Unwin, London.
- [6] Paljug, E., Ohm, T., and Hayati, S., 1995, "The JPL Serpentine Robot: A 12-DOF System for Inspection," Proceedings of the 1995 IEEE International Conference on Robotics and Automation, Nagoya, Japan, May 21–27.
- [7] Klaassen, B., and Paap, K. L., 1999, "GMD-SNAKE2: A Snake-Like Robot Driven by Wheels and a Method for Motion Control," Proceedings of the 1999 IEEE/RSJ International Conference on Intelligent Robots and Systems, Detroit, MI, May 10–15.
- [8] Phee, L., Accoto, D., Menciassi, A., Stefanini, C., Carrozza, M. C., and Dario, P., 2002, "Analysis and Development of Locomotion Devices for the Gastrointestinal Tract," *IEEE Trans. Biomed. Eng.*, **49**(6), p. 613–616.
- [9] Showalter, M., Ingram, M., and Hong, D. W., 2006, "Feasibility Experiments for the Biologically Inspired Whole Skin Locomotion Mechanism," Video Proceedings of the 2006 IEEE International Conference on Robotics and Automation, Orlando, FL, May 15–19.
- [10] Dario, P., Ciarletta, P., Menciassi, A., and Kim, B., 2004, "Modeling and Experimental Validation of the Locomotion of Endoscopic Robots in the Colon," *Int. J. Robot. Res.*, **23**, pp. 549–556.
- [11] Slatkin, A. B., Burdick, J., and Grundfest, W., 1995, "The Development of a Robotic Endoscope," Proceedings of the 1995 IEEE/RSJ International Conference on Intelligent Robots and Systems, Pittsburgh, PA, Aug. 5–9.
- [12] Roh, S., and Choi, H., 2005, "Differential-Drive In-Pipe Robot for Moving Inside Urban Gas Pipelines," *IEEE Trans. Rob. Autom.*, **21**(1), pp. 1–17.
- [13] Breedveld, P., van der Kouwe, D. E., and van Gorp, M. A. J., 2004, "Locomotion Through the Intestine by Means of Rolling Stents," Proceedings of the ASME 2004 Design Engineering Technical Conferences, Salt Lake City, UT, Sept. 28–Oct. 2.
- [14] Flynn, A. M., Udayakumar, K. R., Barrett, D. S., McLurkin, J. D., Franck, D. L., and Shtetman, A. N., 1998, "Tomorrow's Surgery: Micromotors and Microrobots for Minimally Invasive Procedures," *Minimally Invasive Ther. Allied Technol.*, **4**, pp. 343–352.
- [15] Long, G., Anderson, J., and Borenstein, J., 2002, "The Kinematic Design of the OmniPede: A New Approach to Obstacle Traversal," Proceedings of the 2002 IEEE International Conference on Robotics and Automation, Washington, DC, May 11–15, pp. 714–719.
- [16] Schempf, H., 2003, "Aurora: Minimalist Design for Tracked Locomotion," *Robotics Research*, R. A. Jarvis and A. Zemlinsky, eds. Springer-Verlag, Berlin, pp. 453–465.
- [17] Lorch, I. J., 1973, "Some Historical Aspects of Amoeba Studies," *The Biology of Amoeba*, K. W. Jeon, ed., Academic, New York, pp. 1–36.
- [18] Allen, R. D., 1981, "Motility," *J. Cell Biol.*, **91**(3), pp. 148s–155s.
- [19] Taylor, D. L., Condeelis, J. S., Moore, P. L., and Allen, R. D., 1973, "The Contractile Basis of Amoeboid Movement," *J. Cell Biol.*, **59**, pp. 378–394.
- [20] Ecker, A., 1849, "Zur Lehre Vom Bau und Leben der Contractilen Substanz der Niedersten Thiere," *Z. Zellforsch Mikrosk Anat.*, **1**, pp. 218–245.
- [21] Rinaldi, R., and Opas, M., 1976, "Graphs of Contracting Glycerinated Amoeba Proteus," *Nature (London)*, **260**, pp. 525–526.
- [22] Allen, R. D., Cooledge, J. W., and Hall, P. J., 1960, "Streaming in Cytoplasm Dissociated From the Giant Amoeba, *Chaos Chaos*," *Nature (London)*, **187**, pp. 896–899.
- [23] Allen, R. D., Francis, D. W., and Zeh, R., 1971, "Direct Test of the Positive Pressure Gradient Theory of Pseudopod Extension and Retraction in Amoebae," *Science*, **174**, pp. 1237–1240.
- [24] Cullen, K. J., and Allen, R. D., 1980, "A Laser Microbeam Study of Amoeboid Movement," *Exp. Cell Res.*, **128**, pp. 353–362.
- [25] Bar-Cohen, Y., 2001, "EAP History, Current Status, and Infrastructure," *Electroactive Polymer (EAP) Actuators as Artificial Muscles: Reality, Potential, and Challenges*, Y. Bar-Cohen, ed., SPIE—The International Society for Optical Engineering, Bellingham, WA, pp. 3–44.
- [26] Ingram, M., and Hong, D. W., 2006, "Mechanics of the Whole Skin Locomotion Mechanism Concentric Solid Tube Model: The Effects of Geometry and Friction on the Efficiency and Force Transmission Characteristics," Proceedings of the 30th ASME Mechanisms and Robotics Conference, Philadelphia, PA, Sept. 10–13.
- [27] Lahr, D. F., and Hong, D. W., 2008, "The Development of an Incrementally Loaded Finite Element Model of the Whole Skin Locomotion Mechanism: Discovering the Relationship Between Its Shape and Motion," Proceedings of the 32nd ASME Mechanisms and Robotics Conference, New York City, New York, Aug. 3–6.
- [28] Vehar, C., Kota, S., and Dennis, R., 2004, "Closed-Loop Tape Springs as Fully Compliant Mechanisms," Proceedings of the 28th ASME Mechanisms and Robotics Conference, Salt Lake City, Utah, Sept. 28–Oct. 2.
- [29] Pellegrino, S., Kebabdzic, E., Lefort, T., and Watt, A. M., 2002, "Low-Cost Hinge for Deployable Structures," University of Cambridge, Technical Report No. 202.
- [30] Spillers, W. R., Scholgel, M., and Pilla, D., 1992, "A Simple Membrane Finite Element," *Comput. Struct.*, **45**(1), pp. 181–183.
- [31] Schweizerhog, K., and Ekkehard, R., 1984, "Displacement Dependent Pressure Loads in Nonlinear Finite Element Analysis," *Comput. Struct.*, **18**(6), pp. 1099–1114.
- [32] Arcaro, V. F., 2007, "A Simple Procedure for Shape Finding and Analysis of Fabric Structures," <http://www.arcaro.org/tension/index.htm>.